International Journal of Mechanical and Production Engineering Research and Development (IJMPERD)
ISSN (P): 2249-6890; ISSN (E): 2249-8001
Vol. 7, Issue 2, Apr 2017, 221-230

TRANS STELLAR
•Journal Publications •Research Consultancy

PHYSICAL SIMULATION FOR HOT ROLLING POLICY OF ELECTRICAL SI–STEELS

TAHER EL-BITAR, MAHA EL-MELIGY & EMAN EL-SHENAWY

Plastic Deformation Department, Central Metallurgical R&D Institute (CMRDI), Egypt

ABSTRACT

The present work is dealing with three Si-steel alloys. Representative samples were taken and machined from the as- cast ingots to suite the thermo mechanical simulator. The physical simulation process consists of heating to 1100 ºC and then subjected to 5- consecutive hits with different strain at a strain rate 10 sec^{-1}. It was found that the alloys suffer from two contradictory phenomena. The 1st one is dynamic softening due to high strain rate and/or low deformation temperature, while the 2nd phenomenon is the Si sold solution hardening effect. Low Si-content shows pronounced dynamic softening at low deformation temperature (850 ºC) after high (0.44) strain. Medium Si-content appears dynamic softening during the early deformation hits at 1000 ºC and 0.25 strain and continues up to 950 ºC and 0.4 strain, after which hardening appears again. High Si-content launches no pronounced softening during deformation, however, Si sold solution hardening effect becomes prevailing.

KEYWORDS: Electrical Si–Steels, Dilation Curves, Critical Temperature, Thermo-Mechanical Processing, Physical Simulation, Flow Curves & Dynamic Softening

Received: Feb 12, 2017; **Accepted:** Apr 05, 2017; **Published:** Apr 11, 2017; **Paper Id.:** IJMPERDAPR201721

Original Article

INTRODUCTION

Phase transformations in Si-steel alloys play an important role in construction of the hot rolling policy, which would lead to not only the exact targeted dimensions of the sheets, but also would result in microstructure constituents, favoring preferable grain orientations on subsequent processing. The steel chemical composition influences on the phase transformations of the Si-steel. High Si-steel hot rolled sheets usually have coarse grained microstructures, which would enhance shear band formation during subsequent cold rolling [1, 2]. Al plays a similar role as Si on stabilizing the ferrite phase and opposing austenite formation. Sometimes the Si-steel chemical composition is expressed in terms of an equivalent Si content (Si eq =Si+2Al-0.5Mn+0.251P) [2]. On the other hand, carbon increases the gamma constituent of Si steels and detrimentally affects the magnetic properties [2].

Gomes et al. [3] found that the magnetic properties of electrical Si-steels such as permeability and specific losses are, to a large extent, correlated with the microstructure and crystallographic texture. Hot rolling strategies of Si-steel alloys can be classified as austenitic, two-phase, mixed or ferritic rolling. The rough rolling is usually carried out in the austenite region, while the final hot rolling (finish rolling) differs among these routes [4, 5].

On a study to the Influence of deformation process on the improvement of non-oriented electrical steel [4], it was concluded that, a two-phase rolling is preferable for low Si-alloys, however for medium Si-alloys a mixed rolling is better [5], where considerable cube texture components {100} /<001> in the bulk of the material would be created.

Rodriguez-Calvillo et al. [6] found during the physical simulation for hot rolling of the Fe-Si that, increase of the Si-content causes a considerable increase of the flow stress (σf), which would be adversely affected on the rolling force during the hot rolling process. On simulation of high Si-steel by plane strain compression [7], the steel chemical composition was related to the hardening and softening phenomena under hot rolling conditions.

Hot deformation behavior of metals is usually characterized by the simultaneous occurrence of strain hardening and dynamic restoration. Strain hardening is characterized by the multiplication of dislocation density and consequent increase in the internal stress level as the deformation progress. However, the dynamic restoration mechanisms can be divided into recovery and recrystallization [8, 9]. Dynamic recovery (DRv) takes place at any amount of deformation, but its contribution to softening is more intense at the early deformation stages. It is classically associated with metals have a bcc crystallographic structure and high stacking fault energy (SFE) materials, as iron ferrite. On the other hand, many studies reported experimental evidence for the occurrence of dynamic recrystallization in ferritic steel [10, 11]. Dynamic recrystallization in ferritic steel occurs by a mechanism which is different from the classical mechanism of discontinuous dynamic recrystallization (DDRx) observed in low SFE FCC metals. Gourdet et al. [12] suggested that metals with a high SFE can undergo dynamic recrystallization during high temperature deformation by the mechanism of continuous dynamic recrystallization (CDRx). Because of the pronounced dynamic recovery in these metals, new grains are not generated by the standard nucleation mechanism. Instead, low angle boundaries between sub-grains are progressively changed into high angle boundaries by the continuous accumulation of dislocations. This process results in the formation of new equiaxed grains surrounded by high angle boundaries within the deformed original grains.

On the work published by Kang and Torizuka [11], it was concluded that dynamic recrystallization can be obtained by large strain deformation with a high strain rate. Dynamic recrystallization phenomena is usually controlled by Zener- Holloman parameter (Z); $\boldsymbol{Z = \varepsilon^{\cdot} EXP(Q/RT)}$ [13] where, **Q** is the activation energy for hot deformation of Si-steel (276 KJ/ mole) [10], **R** is the gas constant (8.318 J/ mol K), and $\boldsymbol{\varepsilon^{\cdot}}$ is the strain rate (s^{-1}). The grain size of ferrite that can be recrystallized dynamically (d) could be expected by the equation; $\boldsymbol{d = AZ^{-0.16}}$ [11]. i.e, ultra fine grains can be obtained for a large Z-parameter with an increase in the strain rate (**$\boldsymbol{\varepsilon^{\cdot}}$)** even in a high deformation temperature range [11].

The aim of the present article is to construct hot flat rolling policy for the Si-steel alloys under investigation with the aid of thermo-mechanical simulator (Gleeble 3500). The rolling policy depends mainly on conducting deformation in the **γ** region during early steps (rough deformation), while finish rolling passes would be carried on the mixed phase **(α+γ)** region. The simulator is used also for both detecting the transformation temperatures by dilatation and microstructure changes during deformation through five consecutive controlled hits.

EXPERIMENTAL WORK

The steel alloys were processed in an induction melting furnace (100 Kg-capacity). The melt steel was then cast as Y-blocks dimensioned 300 mm length, 200 mm width, and 35 mm thickness. 3 Si-steel alloys were processed with different Si contents and numbered as 21, 22, and 23. The chemical composition of the processed steel alloys is stated in Table 1.

Table 1: Chemical Composition of the Processed Alloys

Alloy	Element, Wt%									Si Equiv.
	C	Si	Mn	P	S	Cu	Al	Cr	Ni	
21	0.0474	0.726	0.174	0.0216	0.0144	0.0382	0.185	0.0447	0.0153	1
22	0.0561	1.46	0.180	0.0220	0.0153	0.0296	0.186	0.0393	0.0165	1.75
23	0.0556	1.95	0.179	0.0216	0.0160	0.0937	0.183	0.0403	0.0137	2.32

The effective part of the Y-block were sectioned and sized into 4 equal sectors. One of the sectors was lath machined into 10 mm diameter bars with 115-120 mm length. The specimens were then screwed from each end to M10 standard screw for 15 mm in accordance with the standard specimens for the thermo-mechanical simulator (Gleeble 3500).

Phase changes taken place during hot deformation were detected by heating (expansion) – cooling (contraction) dilation investigation. Controlled heating during dilation investigation was applied with rates 1.21, 1.3, and 0.45 ^{o}C/sec. up to 1200 ^{o}C, and followed by 30 seconds soaking and then free cooling to room temperature. Phase changes ((α ,α+γ and γ) temperatures can be detected at the inflection points on the dilation curves representing either heating or cooling.

The physical simulation process starts with gradual heating the cylindrical specimens to 1100 ^{o}C then soaking for 12.5 seconds. The heated specimens were subjected to 5- consecutive deformation hits with a strain rate 10 sec^{-1}. Strain rate was chosen as a result of a previous investigation, which emphasizes that 10 sec^{-1} clearly created a pronounced dynamic softening phenomenon [14]. Deformation hits were executed at a temperature range 1100 – 850 ^{o}C. The deformation parameters were selected to simulate the hot rolling conditions of the compact slab process (CSP) followed by direct rolling. The strain during simulation was reduced to about 50% of the actual rolling passes at the CSP process. More details about the deformation parameters during simulation are presented in Figure 1.

The simulation process was designed considering two stages deformation. The 1st stage (rough deformation) contains two consecutive hits, while the 2nd stage (finish rolling) consists of 3 hits. A delay time 20 sec. between roughing and finish deformation stages, to simulate the time usually needed to transfer the steel slab from the roughing stand(s) to the finish rolling stands.

A microstructure investigation has been carried out on cross-section specimens representing different alloys and processing conditions, which would be helpful to explain different phenomenon.

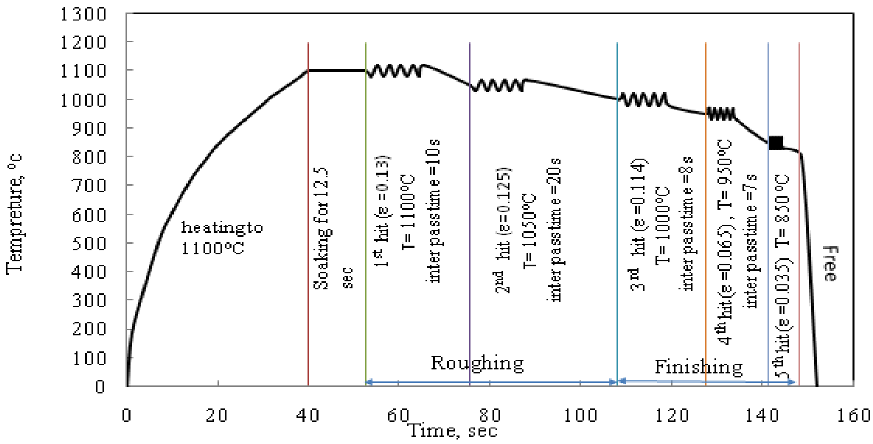

Figure 1: Schematic Presentation of 5 – Consecutive Deformation Hits Carried on the Thermo-Mechanical Simulator (Gleeble 3500)

RESULTS AND DISCUSSIONS

Figure 2 contains the as-cast microstructure of the different Si-steel alloys under investigation.

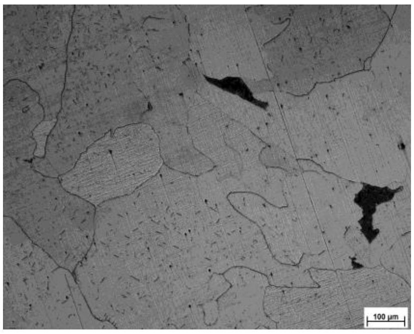

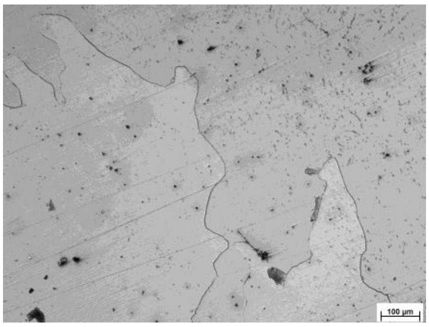

0.726 Si %, X100 **1.46 Si %, X100** **1.95 Si %, X100**

Figure 2: As-Cast Microstructure of the Different Si-Steel Alloys

It is noticed that the microstructure of the low Si-alloy (0.726% Si) consists of mixed fine and coarse grains, while in the medium Si-alloy (1.46 Si %) it contains mostly coarse grains. Furthermore, the microstructure of the high Si-alloy (1.95 Si %) consists of ultra coarse grains.

The microstructure presentations of the 3 alloys reveal the effect of alloying with silicon on enhancing grain coarsening. It is also noticed that the microstructure of the 3 Si-steel alloys contain freckled aggregates. The freckles size and distribution increase with the increase of the Si-content. These freckles were previously identified as Fe-Si carbides [15], having a chemical composition as; $Fe_{10}Si_2C_3$.

The Fe-Si alloys have a special feature on their binary phase diagram. The left hand side of the Fe-Si phase diagram contains usually a closed region of austenite (γ), which is surrounded by austenite + ferrite (γ + α) loop and followed by a region of ferrite (α). Consequently, the dilation curves of the alloys under investigation, could contain more than one inflection point representing passing of each alloy through the region of γ and crossing the loop of γ + α.

Heating (expansion) dilation curves are presented in Figure 3 for alloy 21, Figure 4 for alloy 22 and Figure 5 for alloy 23. It is clear from the dilation curves that the 3 alloys under investigation are existing on the left hand side (Fe-rich) portion of Fe-Si phase diagram and passing through the closed γ region during heating. Furthermore, each Si –alloy crosses the loop of mixed γ + α two times. The exact crossing temperatures of each alloy can be detected at the inflection points on the dilation curves.

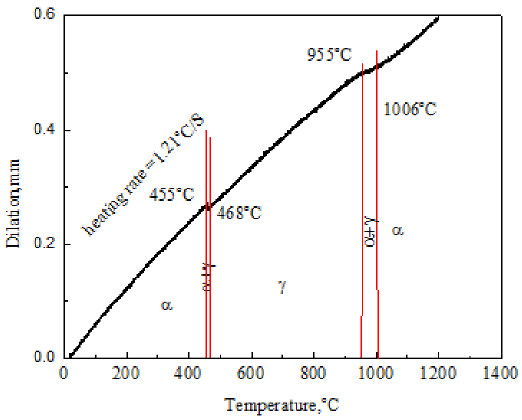

Figure 3: Dilation Curve for Alloy 21

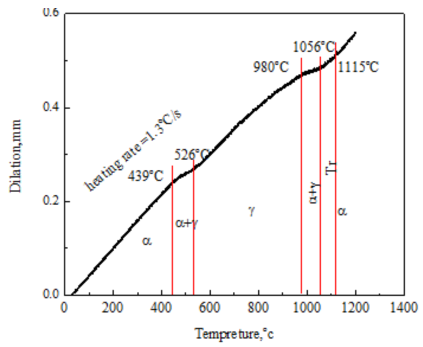

Figure 4: Dilation Curve for Alloy 22

In Figure 5, heating of alloy 23 with a low rate (0.45 ºC/s) shows early inflection on the dilation curve at temperature range 110- 200 ºC. This early inflection represents magnetic transformation behavior of the alloy, where a two phase field (B2 + DO3) is stable [16].

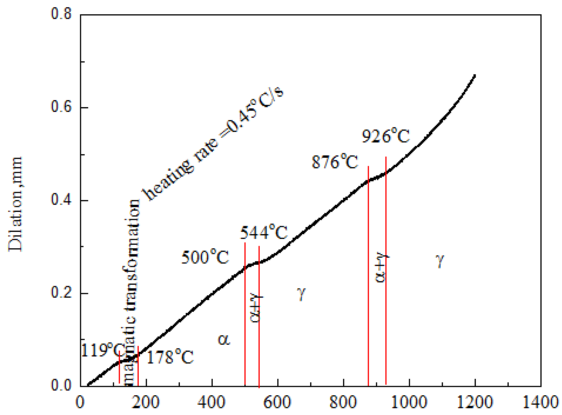

Figure 5: Dilation Curve for Alloy 23

Figure 6 represents the closed region of γ along with the loop of mixed γ + α for the alloys under investigation. Figure 6 is important for the construction of the hot rolling policy. Pre-rolling (rough rolling stage) should be undertaken in the austenite region [3], while the final hot rolling (finish rolling) would be carried out as mixed phase rolling, where considerable cube texture components {100} /<001> in the bulk of the material would be created [4].

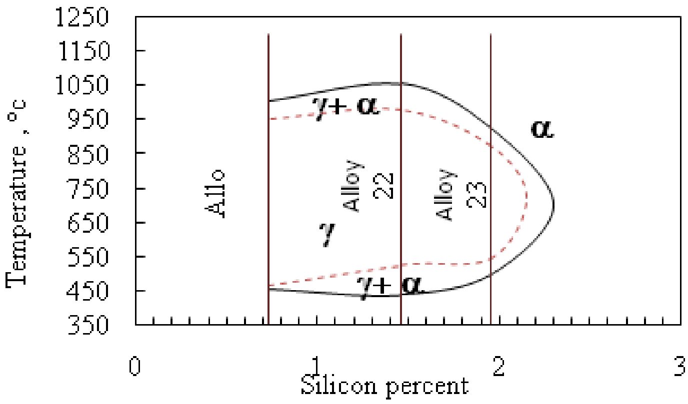

Figure 6: Closed Region of Γ Along with the Loop of Mixed Γ + A for the Alloys under Investigation

The simulation process creates 5-consecutive stress-strain curves representing the 5-consecutive hits. Figure 7 represents the consecutive stress-strain relationships for alloy 21 under high-strain rate (10 s^{-1}). Generally, for each curve, the stress increases linearly at the beginning (proportional stress- strain), followed by stepwise (curved) increase in stress with strain. The end of the proportional stress – strain relationship determines the flow stress (**σf**).

The flow stresses of different curves represent the flow curve. The flow curve of alloy 21 deformed with a high strain rate (10 s^{-1}) is presented in Figure 8. The flow curve appears continuous increase of **σf** from a hit to the other as a result of continuous accumulation of dislocations [12] (strain hardening effect) due to the continuous decrease of deformation temperature up to hit No. 4, at a total strain 0.41 and 950 °C. On hit No. 5, by increasing the total strain to 0.44 at temperature 850 °C (< **Tr**), the flow stress (**σf**) decreases however considerably, which is a consort for dynamic softening [10, 11]. Dynamic recrystallization is usually controlled by Zener- Holloman parameter (Z). Considering the values of Q, R, T, and ε [13], the Z-parameter is calculated as Ln Z = 28.46. High values of Z ensure that dynamic recrystallization would be taken place, where high strain rate and low deformation temperature would be attained, which is the case of hit no. 5.

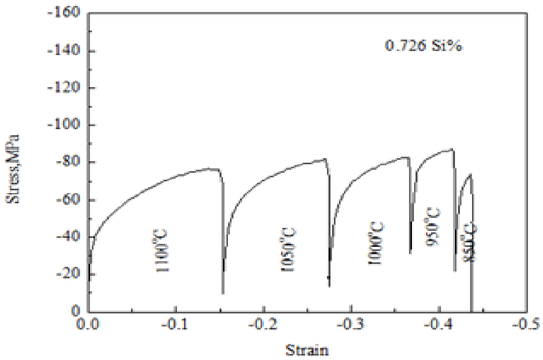

Figure 7: 5-Consecutive Stress-Strain Curves for Alloy 21 under 10 S^{-1} Strain Rate

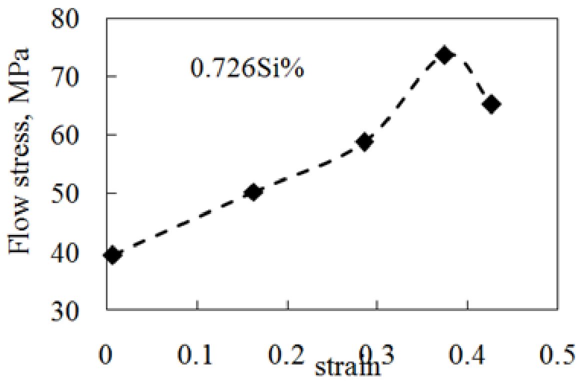

Figure 8: Flow Curve of Alloy 21 under 10 S^{-1} Strain Rate

Similarly, the 5-consecutive stress-strain curves of alloy 22 (1.46 Si %) are presented in Figure 9. The flow stresses behavior is presented as a flow curve in Figure 10. Dynamic softening of alloy 22 appears early after hit no. 2 and continues up to hit no. 4. On hit no. 5, hardening appears again, where the effect of the Si-content becomes predominant [15] during last hit, at a low deformation temperature (850 ºC).

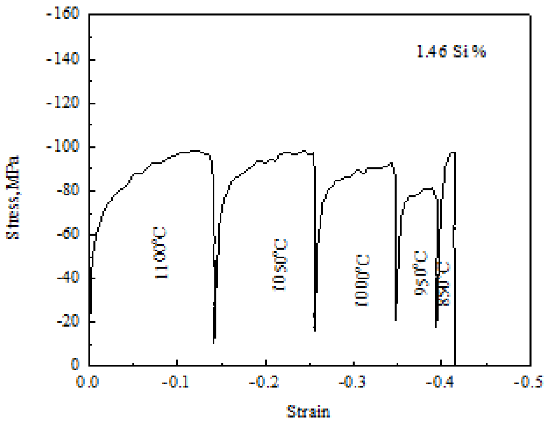

Figure 9: 5-Consecutive Stress-Strain Curves for Alloy under 10 S^{-1} Strain Rate

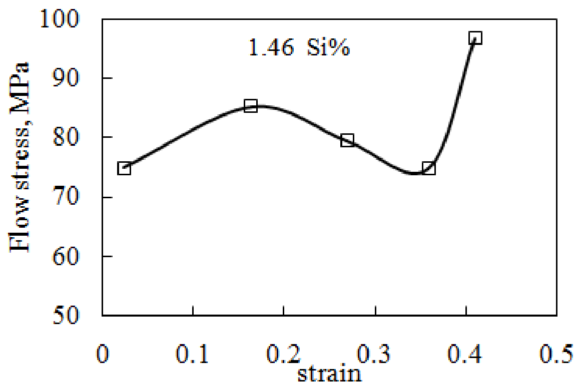

Figure 10: Flow Curve of Alloy 22 under 10 S^{-1} Strain Rate

On the other hand, physical simulation of the high Si-content alloy (no. 23) is presented as 5-consecutive stress-strain relationships in Figure 11. The flow curve of alloy 23 which is presented in Figure 12 appears similar behavior as in alloy 22, but softening after the 2nd hit is not pronounced as in alloy 22. In high Si-steel alloys, Si plays a considerable role as a sold solution hardener. Consequently, two contradictory effects are present. 1st effect is dynamic softening due to high strain rate, while the 2nd effect is the Si sold solution hardening. On the last simulation hit (no. 5), the Si sold solution hardening effect becomes prevailing.

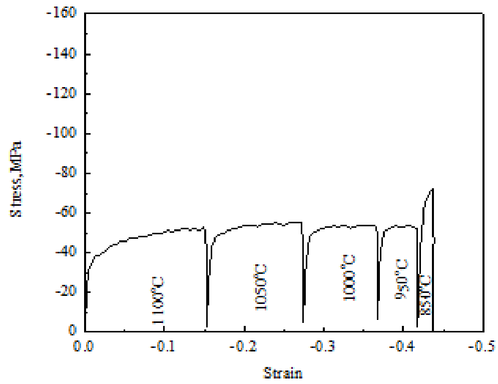

Figure 11: 5-Consecutive Stress-Strain Curves for Alloy 23 under 10 S^{-1} Strain Rate

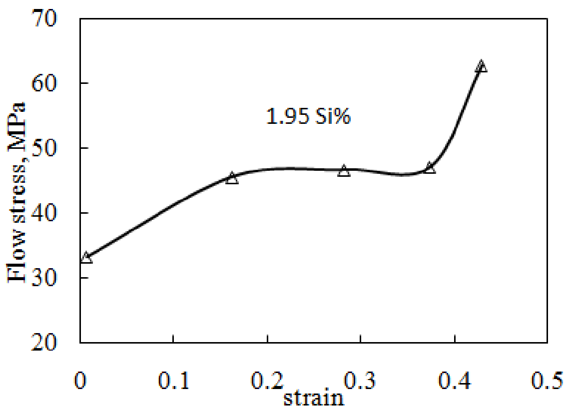

Figure 12: Flow Curve of Alloy 23 under 10 S^{-1} Strain Rate

Figure 13 shows representive microstructure, taken from the physical simulations specimens of the 3 alloys after deformation with a high strain rate (10 s^{-1}). The different microstructures contain ferrite grains sourounded by thin layers of austenite phase. The 3 specimens were subjected to grain refinement, to a certain extent, as a result of dynamic softening in selected areas. It is also noticed that selected coarse grains were considerably found especially in alloy 23, as a result of containing high silicon.

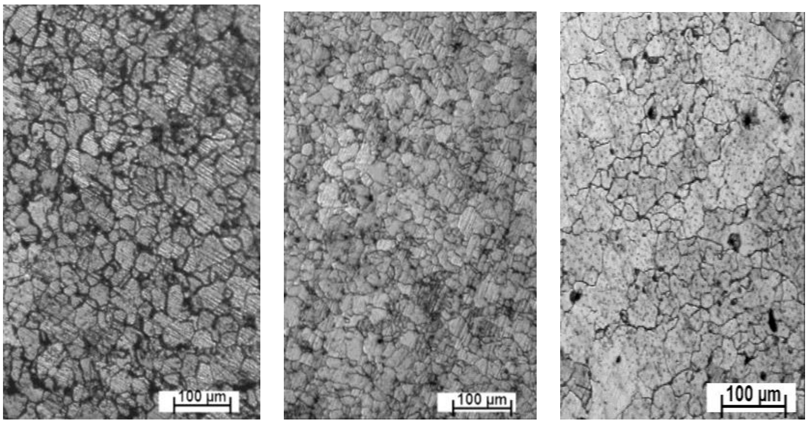

Si 21 x 100 **Si 22 x100** **Si 23 x100**

Figure 13: Representive Microstructureof the Physical Simulations Specimens of the 3 Alloys at a High Strain Rate (10 S^{-1}).

CONCLUSIONS

- Alloying with Si affects on the ferrite grain coarsening.
- The 3 alloys are passing through the closed region **of γ** during heating and cross the loop of mixed γ + α two times.
- During the simulation process, 1st two hits were conducted as a pre-deformation stage in the austenite region, while the final three hits were carried out as mixed phase rolling.
- During hot deformation, the Si-steel poses two contradictory phenomenons. The 1st one is dynamic softening due to high strain rate and/or low deformation temperature, while the 2nd phenomena is the Si sold solution hardening effect.
- Low Si-content (alloy 21) shows pronounced dynamic softening at low deformation temperature (850 ºC) and high (0.44) strain.
- Medium Si-content (alloy 22) appears dynamic softening during the early deformation hits at 1000 ºC and 0.25 strain and continues up to 950 ºC and 0.4 strain, after which hardening appears again, where the effect of the Si-content becomes predominant.
- High Si-content (alloy 23) launches no pronounced softening during deformation, however, Si sold solution hardening effect becomes prevailing.

ACKNOWLEDGMENTS

The current work is a part of a project supported financially by the Science and Technology Development Fund (STDF), Egypt, Grant No 7991. The authors acknowledge this generous assistance.

REFERENCES

1. *Huneus H, Günther K, Kochmann T, Plutniok V and Schop A 1993 Nonoriented magnetic steel with improved texture and permeability Journal of Material Engineering Performenc **2** 199-203*
2. *Sidora J J, Verbeken K, Gomes E, Schneider J, Calvillo P R and Kestens L A 2012 Through process texture evolution and magnetic properties of high Si non-oriented electrical steels Material Characterization **71** 49-57*
3. *Gomes E, Schneider J, Verbeken K, Hermann H and Houbaert Y 2010 Effect of hot and cold rolling on grain size and texture in Fe–Si strips with Si-content larger than 2 wt.% Material Science Forum **638-642** 3561-6*
4. *Fischer O and Schneider J 2003 Influence of deformation process on the improvement of non-oriented electrical steel Journal of Magnetism and Magnetic Materials **254-255** 302-306*
5. *Friedrich K E, Hammer B, Kawalla R, Pircher H, Schneider J, Fischer O and Wuppermann C D 2000 Non-textured Electrical Steel Sheet, Useful For Cores In Rotary Electrical Machines Such As Motors And Generators, Is Produced By Multi-pass Hot Rolling Mainly In The Two-phase Austenite-ferrite Region German Patent DE 19930519*
6. *Calvillo P Rodriguez, Boulaajaj A, Perez-Sine M, Schneider J and Cabrera J 2014 On the hot working of FeSi ferritic steels Materials Science & Engineering A **606** 127-138*
7. *Calvillo P Rodriguez, Yanes T Ros, Ruiz D, Colas R and Houbaert Y 2006 Plane strain compression of high silicon steel Material Science and Technolgy **22** 1105-1111*
8. *Humphreys F and Hatherly M 2004 Recrystallization and Related Annealing Phenomena, (Oxford: Elsevier) 169-319*
9. *McQueen H J and Ryan N D 2002 Constitutive analysis in hot working Materials Science & Engineering A **322** 43-63*
10. *Han K S, Song T J and Charles D C B 2013 Hot Deformation Behavior of Fe-2%Si International Journal of Iron and Steel Institute of Japan **53** 294-303*
11. *Kang J and Torizuka S 2007 Dynamic recrystallization by large strain deformation with a high strain rate in an ultralow carbon steel Scripta Materialia **57**(11) 1048-1051*
12. *Gourdet S and Montheillet F 2003 Acta Materialia A model of continuous dynamic recrystallization **51** 2685-99*
13. *Medina S F and Hernandez C A 1996 General expression of the Zener-Hollomon parameter as a function of the chemical composition of low alloy and microalloyed steels Acta Materialia **44**(1) 137-148*
14. *El-Bitar T, El-Meligy M and El-Shenawy E 2015 Detection of dynamic softening duringhot deformation of medium Si-steels by a thermo- mechanical simulator (Gleeble 3500) International Journal of Mechanical and Production Engineering Research and Development **5** 65-74*
15. *El-Bitar T, Funke P, Mekkawy M and Mohamed K 1992 Conduct of Si-steel Alloys under conditions of Hot-rolling The Processing, Properties and Applications of Metallic and Ceramic Materials conference (Birmingham U.K.) Material & Component Engineering Puplications LTD.,UK 1031-36*
16. *Kubaschewski O 1982 Iron- Silicon IRON—Binary Phase Diagrams (Berlin –Heidelberg) Springer-Verlag Berlin Heidelberg 136-139*